Development 140, 1457-1466 (2013) doi:10.1242/dev.086850

Jun N-terminal kinase maintains tissue integrity during cell rearrangement in the gut

Michael K. Dush and Nanette M. Nascone-Yoder*

SUMMARY

Tissue elongation is a fundamental morphogenetic process that generates the proper anatomical topology of the body plan and vital organs. In many elongating embryonic structures, tissue lengthening is driven by Rho family GTPase-mediated cell rearrangement. During this dynamic process, the mechanisms that modulate intercellular adhesion to allow individual cells to change position without compromising structural integrity are not well understood. In vertebrates, Jun N-terminal kinase (JNK) is also required for tissue elongation, but the precise cellular role of JNK in this context has remained elusive. Here, we show that JNK activity is indispensable for the rearrangement of endoderm cells that underlies the elongation of the *Xenopus* gut tube. Whereas Rho kinase is necessary to induce cell intercalation and remodel adhesive contacts, we have found that JNK is required to maintain cell-cell adhesion and establish parallel microtubule arrays; without JNK activity, the reorganizing endoderm dissociates. Depleting polymerized microtubules phenocopies this effect of JNK inhibition on endoderm morphogenesis, consistent with a model in which JNK regulates microtubule architecture to preserve adhesive contacts between rearranging gut cells. Thus, in contrast to Rho kinase, which generates actomyosin-based tension and cell movement, JNK signaling is required to establish microtubule stability and maintain tissue cohesion; both factors are required to achieve proper cell rearrangement and gut extension. This model of gut elongation has implications not only for the etiology of digestive tract defects, but sheds new light on the means by which intra- and intercellular forces are balanced to promote topological change, while preserving structural integrity, in numerous morphogenetic contexts.

KEY WORDS: JNK, Rho kinase, Endoderm, Gut, Intestine, Morphogenesis, *Xenopus*

INTRODUCTION

The primitive gut tube of the vertebrate embryo must elongate extensively to generate the requisite dimensions and configuration of the mature digestive tract. The final length of the gut determines its overall functionality and constrains the surface area of the epithelial lining, impacting not only normal digestive capacity but also the ability to adapt to disease or dietary change (Karasov and Diamond, 1988; Stainier, 2005; Weaver et al., 1991). Therefore, understanding the mechanisms that drive primitive gut tube elongation has biomedical, evolutionary and ecological implications.

In diverse species, signaling via non-canonical Wnt and/or planar cell polarity (Wnt/PCP) pathways drives tissue lengthening by orchestrating the reorganization of an initially wide field of cells into a narrower, and thus longer, array; this process is referred to as 'convergent extension' during gastrulation (Bartolini and Gundersen, 2006; Jones and Chen, 2007; Keller, 2002). Recent evidence also implicates Wnt/PCP signaling in gut tube elongation, as mice lacking the Wnt/PCP ligand *Wnt5a* (Cervantes et al., 2009), the non-canonical Wnt/PCP receptor *Ror2* (Yamada et al., 2010) or antagonists of non-canonical Wnt signaling, the *Secreted-Frizzled-Related Proteins* (*Sfrps*) (Matsuyama et al., 2009), all exhibit a dramatic shortening of the intestine.

Although multiple Wnt/PCP signaling components are essential for the proper lengthening of the gut, the downstream morphogenetic events that drive gut tube elongation are still unresolved. In other contexts, Wnt/PCP signaling controls tissue extension by regulating cell polarity, adhesion and/or cytoskeletal dynamics to induce cell rearrangements (Keller, 2002; Marlow et al., 2002; Roszko et al., 2009; Yin et al., 2008). Similar morphogenetic properties and processes are implicated in mammalian gut elongation, as suggested by the abnormal polarity and/or stratification of the intestinal epithelium observed in Wnt/PCP mutant mice (Cervantes et al., 2009; Matsuyama et al., 2009; Yamada et al., 2010). Moreover, the definitive (gut-forming) endoderm undergoes convergent extension rearrangements prior to formation of the gut tube (García-García et al., 2008) and it has been hypothesized that endoderm cells in the gut tube itself also rearrange in order for the tube to narrow as it lengthens (Matsumoto et al., 2002; Yamada et al., 2010). However, during later stages of development, transformation of the pseudostratified architecture of the primitive gut lining into a less densely packed mature epithelium has also been postulated to contribute to lengthening (Grosse et al., 2011). Although the exact cellular and molecular events that orchestrate this crucial process remain equivocal, these observations all implicate various phases in the morphogenesis of the endodermal epithelium in the elongation of the embryonic digestive tract.

In the *Xenopus laevis* embryo, endoderm cells initially fill the primitive gut tube, but then become apicobasally polarized and radially intercalate between their neighbors to generate a central lumen (see Fig. 1) (Chalmers and Slack, 2000; Reed et al., 2009). Cell labeling and fate-mapping studies have shown that, as these intercalating cells gradually resolve into a single layer epithelium, they become distributed in a narrow line along the longitudinal axis of the lengthening gut tube (Chalmers and Slack, 2000; Muller et al., 2003; Reed et al., 2009). Thus, radial rearrangements in the endoderm occur in a polarized manner to not only thin the gut lining, but also to drive tissue extension, similar to the role of radial intercalation during gastrulation (Roszko et al., 2009). Consistent

Department of Molecular Biomedical Sciences, Center for Comparative Medicine and Translational Research, College of Veterinary Medicine, North Carolina State University, 1051 William Moore Drive, Raleigh, NC 27606, USA.

*Author for correspondence (nmnascon@ncsu.edu)

Accepted 23 January 2013

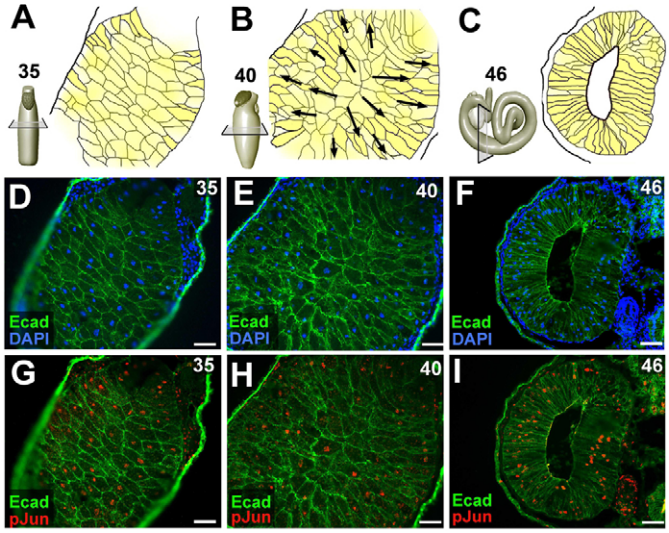

Fig. 1. JNK is active in the rearranging endoderm during *Xenopus* gut elongation. (**A-C**) Endoderm morphogenesis is depicted in representative sections of the midgut during three stages of gut elongation. At stage 35 (A), the endoderm cells (yellow) of the primitive gut tube have not yet aligned along the apicobasal axis of the gut tube. By stage 40 (B), most of the endoderm cells have become apicobasally aligned. Over subsequent stages, the endoderm cells radially intercalate, as indicated by the black arrows, opening the central lumen, forming the digestive epithelium and driving gut tube elongation. At stage 46 (C), a mature endoderm epithelium lines the fully elongated gut tube. (**D-I**) Immunohistochemical staining reveals E-cadherin (Ecad, green) and nuclei (blue) or phosphorylated Jun (pJun, red), as indicated. JNK activity is indicated by the accumulation of pJun in the endoderm nuclei at all stages. Scale bars: 50 μm.

with this model, perturbing actomyosin contractility by inhibiting Wnt/PCP effectors, including the small GTPase Rho, Rho-associated kinase or nonmuscle Myosin II, results in dramatically shortened guts occluded with layers of unintercalated endoderm (Reed et al., 2009).

Activation of Jun N-terminal kinase (JNK) is also an established downstream effect of Wnt/PCP signaling (van Amerongen and Nusse, 2009; Boutros et al., 1998). JNK is essential for convergent extension during gastrulation (Carron et al., 2005; Kim and Han, 2005; Yamanaka et al., 2002) and JNK activation, as indicated by phosphorylation of JNK and/or Jun, correlates with tissue lengthening in both gastrulating tissues and Wnt/PCP mutant guts (Habas et al., 2003; Li et al., 2008; Matsuyama et al., 2009). However, in contrast to Rho, the actomyosin-based force-producing roles of which are well established (Narumiya et al., 2009), the potential cellular function of JNK during tissue elongation has not been elucidated.

In this study, we investigated the role of JNK in *Xenopus* gut tube elongation, providing new insight into the molecular and cellular processes that enable the morphogenesis of a properly elongated digestive tract. We find that JNK is required to establish microtubule architecture and maintain intercellular adhesion in the intercalating endoderm. Hence, Rho kinase and JNK play complementary roles during tissue elongation, balancing the contractile forces that drive cell rearrangement with mechanisms that maintain overall structural integrity. As these signaling pathways operate downstream of Wnt/PCP signaling in numerous developmental contexts, our model of gut morphogenesis has larger implications for a variety of cell rearrangement events that shape elongated tubes, epithelial organs and body plans.

MATERIALS AND METHODS

Embryos and inhibitor dosing

Xenopus laevis embryos were obtained by *in vitro* fertilization, de-jellied with 2% cysteine-HCl (pH 7.8-8.1), sorted to eliminate individuals with developmental anomalies and cultured in 0.1× Marc's Modified Ringers at 15-22°C (Sive et al., 1998). Staging was according to Nieuwkoop and Faber (Nieuwkoop and Faber, 1994). Embryos were exposed to small-molecule inhibitors (10-40 μM SP600125, 20-80 μM Rockout, 15 μg/ml nocodozole or 1 μM epothilone B; Calbiochem), or the equivalent volume of DMSO. Tadpoles (stage 41-46) were anesthetized in 0.05% MS222 for morphological analysis, dissections and/or fixation.

Morpholino knockdown

Morpholino oligonucleotides (GeneTools) targeted the translation start site of *X. laevis JNK 1* (5′-TGCTGTCACGCTTGCTTCGGCTCAT-3′), or a standard control sequence that targets a splice mutant of human β-globin, 5′-CCTCTTACCTCAGTTACAATTTATA-3′). A pCS2 construct encoding mCherry-CAAX was linearized with *Not*I and capped mRNA was synthesized with the mMessage Machine kit (Ambion), and purified using NucAway columns (Ambion). Synthetic mRNA and/or morpholinos (3.4 ng/injection) were co-injected into the ventrovegetal blastomeres of 8- to 16-cell stage embryos as described previously (Reed et al., 2009).

Gut cell dissociation-reaggregation assays

Whole gut tubes were dissected from DMSO, Rockout and SP600125-treated embryos (n=10 each), rinsed in calcium- and magnesium-free medium (CMF; Sive et al., 2007), transferred to agarose-coated dishes containing CMF, and dissociated with gentle agitation on an orbital shaker at 100 rpm. For reaggregation, the single cell suspension was supplemented with $CaCl_2$ to restore Ca^{2+}-dependent adhesion. Multicellular reaggregates formed after 90 minutes, and the pixel area of individual clusters of more than three cells was used to indicate cluster size and adhesion strength.

Cell rearrangement

Devitellinized stage 23-24 embryos were microinjected at various depths into the prospective gut tube (Muller et al., 2003) with ~30 pl of DiI and/or DiO solution (Vybrant DiI/ DiO, Invitrogen). To assess radial rearrangement patterns, embryos were fixed for 30 minutes in PBS containing 3.7% formaldehyde, 0.25% glutaraldehyde and 0.1% Tween 20, and sectioned transversely with a razor blade. The resulting 350-700 μm tissue slabs were washed three times with PBS containing 0.1% Tween 20 (PBT), then incubated overnight at 4°C in Alexa 488-phalloidin (Invitrogen; 5 units/ml in PBT) to visualize cortical actin as an indicator of cell shape (Nandadasa et al., 2009). The slabs were washed three times for 1 hour with PBT, and imaged *en face* using a Leica SPE II confocal microscope. To quantify longitudinal cell rearrangement patterns, the guts from embryos injected with lipophilic dyes were isolated and flat-mounted under a coverslip fragment for imaging (Zeiss LUMAR stereomicroscope). The length and width of the DiI and/or DiO-labeled cell populations were measured in at least six guts (Photoshop Measure tool) and the average length-to-width ratio of the labeled area was calculated.

Gene expression

Whole gut tubes were dissected at stage 42-46, fixed in MEMFA (Sive et al., 1998) and gradually dehydrated through several changes of ethanol. Digoxigenin-labeled riboprobes derived from the coding regions of *Xenopus Nkx-2.5*, *Pdx1*, *Hhex* and *IFABP* were synthesized from linearized plasmids (Muller et al., 2003) (gifts from P. Krieg, University of Arizona, Tucson, AZ, USA; and C. Wright, Vanderbilt University, Nashville, TN, USA), and *in situ* hybridization was carried out on isolated guts as described previously (Lipscomb et al., 2006).

Immunohistochemistry

Whole embryos were fixed for 45 minutes in 4% PFA [100 mM Hepes (pH 7.4), 100 mM NaCl, 4% paraformaldehyde], followed by five washes in −20°C Dent's fixative (80% methanol/20% DMSO). After overnight storage, embryos were rinsed and incubated for 1 hour in Tris-NaCl (100 mM Tris HCl pH 7.3, 100 mM NaCl) before transfer to sucrose/gelatin (15% sucrose/25% cold-water fish gelatin) overnight. Embryos were embedded in

OCT (Tissue-Tek), sectioned at 10 μm and picked up on coated slides (Fisher Superfrost). Sections were post-fixed in acetone for 1 minute and blocked for 30 minutes as described previously (Reed et al., 2009). Immunohistochemical staining was achieved by overnight incubation at 4°C in blocking buffer containing primary antibodies against the following proteins: phosphoJun (Cell Signaling, 9261; 1:100), E-cadherin (DSHB, 5D3; 1:200), laminin (Sigma, L9393; 1:200), β-catenin (SCBT, H-102; 1:100), aPKC (Santa Cruz, sc216; 1:200-1:250), α-tubulin (Sigma, T9026; 1:1000), active caspase 3 (Abcam, ab13847; 1:200), mCherry (Clontech, 632543; 1:500-1:1000), smooth muscle actin (Sigma, A5228; 1:1000) and phospho-histone H3 (Upstate, 06-570; 1:1000). Slides were then washed twice in PBT for 5 minutes, incubated for 3 hours in blocking buffer containing Alexa 488-conjugated goat anti-mouse IgG (Invitrogen, A11029; 1:2000) and/or Alexa 546-conjugated goat anti-rabbit IgG (Invitrogen, A11035; 1:2000), and washed in PBT. Autofluorescence was quenched in Eriochrome Black (0.2% w/v in PBS, 5 minutes). Quenched slides were washed in PBS, mounted in Prolong Gold (or Prolong Gold with DAPI), cured overnight in the dark, and sealed with nail polish. Fluorescence was visualized on a Leica DM5000B or Leica SPEII confocal microscope.

Western blots and JNK activity assays

Whole guts were isolated and placed in ice-cold RIPA (ThermoScientific) buffer containing protease and phosphatase inhibitors (Halt Protease and Phosphatase Cocktail; Pierce), homogenized by manual pipetting and frozen at −80°C. Three freeze/thaw cycles were performed, and the cell debris was pelleted by centrifugation at 16,000 ***g*** at 4°C for 15 minutes. The protein concentration of the gut lysate was determined (Pierce BCA Protein Assay Kit) and 10-20 μg of total protein was run on a NuPage 4-12% Bis-Tris gel (Invitrogen) and electrophoretically transferred to a PVDF membrane (Invitrogen). The membrane was blocked for 30 minutes with PBT containing 5% non-fat dry milk, and incubated overnight at 4°C in PBT containing 5% non-fat dry milk or 5% BSA and primary antibodies against E-cadherin (DSHB, 5D3; 1:1000), β-catenin (Sigma, C-2206; 1:500), α-catenin (Abcam, ab11346; 1:500), JNK1 (Santa Cruz Biotechnology, sc-571; 1:200) and/or ERK (Cell Signaling, 9102; 1:1000). Membranes were washed in PBT and incubated for 1 hour with a horseradish peroxidase-conjugated donkey anti-mouse (Jackson, 715-035-150; 1:2000), or donkey anti-rabbit secondary antibody (Jackson, 711-035-152; 1:2000). Signals were detected by enhanced chemiluminescence (Pierce ECL). JNK activity assays (phosphoJun levels) were performed using a SAPK/JNK Kinase Assay kit (Cell Signaling Technology).

RESULTS

JNK is active in the *Xenopus* gut endoderm

During the morphogenesis of the *Xenopus* digestive tract, the endoderm cells in the primitive gut tube gradually adopt an apicobasal orientation. The cells then radially intercalate between their neighbors to generate a lumen and form a mature epithelium, concomitantly narrowing and lengthening the gut tube (Fig. 1A-F; Reed et al., 2009). To assess JNK activity in the rearranging endoderm during this process, we used immunohistochemical staining to detect nuclear accumulation of phosphorylated Jun (pJun) in sections of the developing gut tube. JNK activity is found throughout the endoderm during *Xenopus* gut elongation (Fig. 1G-I).

JNK is required for gut tube elongation but not for gut patterning

To determine the role of JNK during gut morphogenesis, we exposed developing *Xenopus* embryos to SP600125, a potent pharmacological inhibitor of JNK (Bennett et al., 2001), from a stage prior to the majority of endoderm cell shape change and intercalation (stage 35; see Fig. 1A) through to stage 46, when the primitive gut tube has fully elongated into a coiled tadpole intestine (see Fig. 1C). The inhibitor eliminates most JNK activity in the gut, as indicated by dramatically decreased phosphoJun levels in gut tube extracts from SP600125-exposed embryos (inset, Fig. 2B).

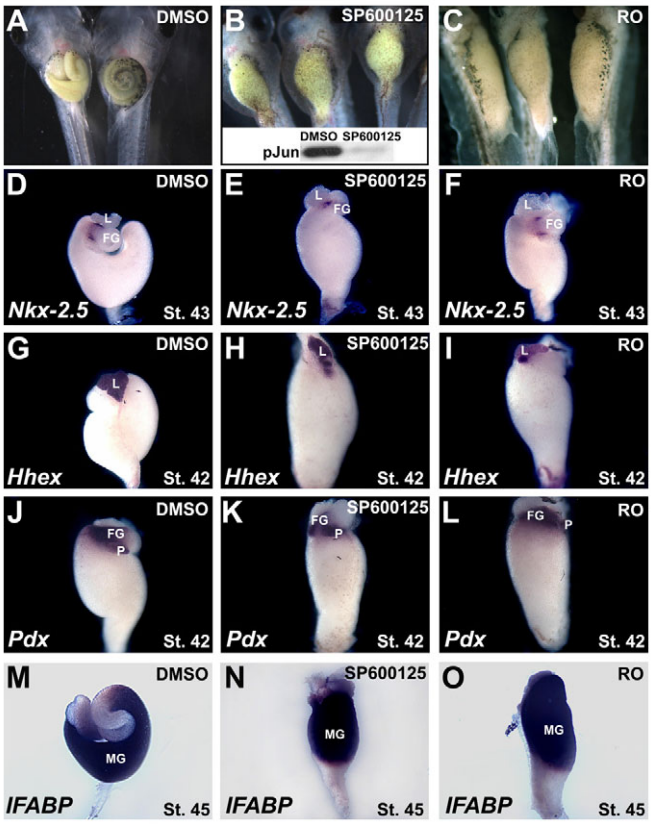

Fig. 2. JNK is required for gut tube elongation, but not for digestive organ patterning. (**A-C**) Embryos were exposed to DMSO, SP600125 or Rockout (RO) from stage 35. Compared with the long coiled intestine in stage 46 DMSO controls (A), gut elongation is severely disrupted in embryos exposed to SP600125 (B) and RO (C). Decreased phosphoJun (pJun) levels in stage 46 gut extracts (inset, B) confirm the efficacy of JNK inhibition in the gut by SP600125. The efficacy of Rockout (~74% reduction in Rho kinase activity) was confirmed using a Rho-kinase Assay Kit (Cyclex; not shown). (**D-O**) Gut-specific gene expression patterns were assessed by *in situ* hybridization in developing gut tubes isolated at stage 43 (D-F), 42 (G-L) or 45 (M-O). Appropriate region- and tissue-specific expression of *Nkx-2.5* (D-F; mesoderm boundary between stomach and duodenum), *Hhex* (G-I; liver; G is shown in dorsal view), *Pdx* (J-L; pancreas and duodenal endoderm) and *IFABP* (M-O; intestinal endoderm) is evident under all conditions (*n*=6-17). FG, foregut; L, liver; MG, midgut; P, pancreas.

Compared with DMSO controls, SP600125-exposed guts exhibit severe elongation defects, similar to embryos exposed to Rockout (RO), an inhibitor of Rho-associated kinase (Fig. 2A-C). Importantly, SP600125 inhibits lengthening while preserving the appropriate (albeit compressed) region-specific expression of a variety of gut patterning markers (compare Fig. 2D,G,J,M with 2E,H,K,N, respectively), as also observed in RO-treated embryos (Fig. 2F,I,L,O). These results confirm that the SP600125-induced short gut phenotype results not from patterning defects in the gut tube, but from a failure of the morphogenetic processes that lead to gut elongation. Thus, both Rho kinase and JNK are required for tissue elongation in the *Xenopus* gut tube.

JNK is required for endoderm cell rearrangements

Previous reports indicate that *Xenopus* endoderm cells undergo extensive rearrangement during gut morphogenesis, in both radial

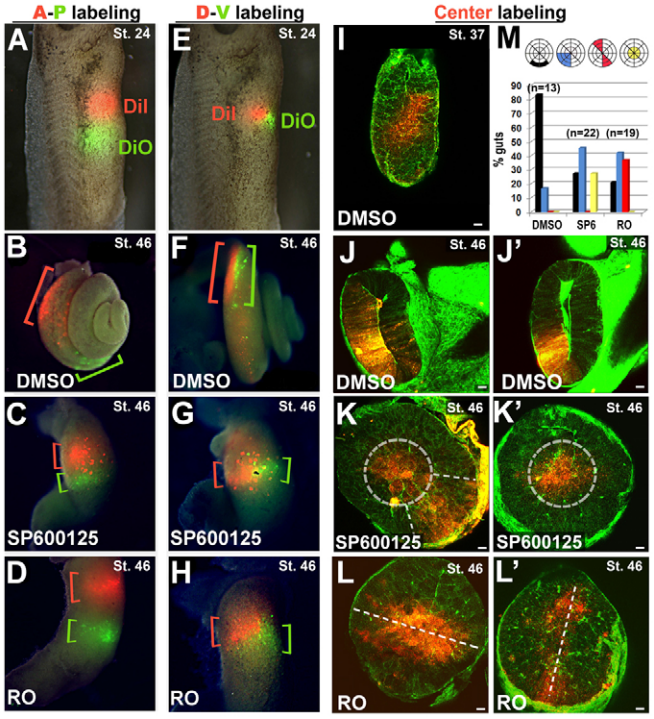

Fig. 3. JNK is required for endoderm cell rearrangements. (**A-H**) The prospective gut endoderm was injected with two lipophilic dyes (DiI, red; DiO, green) in anterior-posterior (A-P labeling; A-D) or dorsal-ventral (D-V labeling; E-H) orientations at stage 24. Labeled embryos were exposed to DMSO (B,F), SP600125 (C,G) or Rockout, RO (D,H), from stage 35-46; whole guts were dissected to visualize the final longitudinal distribution of each dye (indicated by red or green brackets). Labeled cells become distributed along the axis of the gut tube in DMSO controls (B,F), but fail to rearrange in the presence of SP600125 (C,G) or Rockout (D,H). (**I-L′**) Deep endoderm cells of the prospective gut tube were injected with DiI (red) at stage 24 to achieve 'Center labeling', as shown (I, stage 37). Labeled embryos were then exposed to DMSO (J,J′), SP600125 (K,K′) or RO (L,L′) from stages 35 to 46, bisected and counterstained with phalloidin (green). In DMSO controls (J,J′), the labeled cells have radially intercalated and are incorporated within the gut epithelium. In the presence of SP600125, labeled cells are confined to a central 'core' of endoderm (dashed circles in K.K′) or to a radial quadrant of stratified cells (dashed lines in K). In the presence of RO, labeled cells span the entire diameter of the tube (L,L′). (**M**) The frequency of individual guts with the DiI label contacting only the basement membrane (black), occupying a radial quadrant of the gut tube (blue), spanning the gut diameter (red) or confined only to the center (yellow) after exposure to DMSO, SP600125 or RO. Scale bars: 50 μm.

and longitudinal directions (Chalmers and Slack, 2000; Reed et al., 2009). To compare the roles of Rho kinase and JNK in these multidimensional rearrangements, we labeled small populations of endoderm cells with lipophilic dyes and then assessed their final patterns.

First, to assess longitudinal redistribution, we labeled neighboring populations of cells with both DiI and DiO (Fig. 3A,E), and then exposed labeled embryos to DMSO, RO or SP600125. The expected redistribution of labeled cells in a narrow line along the longitudinal axis of the gut tube, as exhibited in DMSO controls (Fig. 3B,F), is severely curtailed in the presence of SP600125 (Fig. 3C,G) and RO (Fig. 3D,H), consistent with the short gut phenotypes induced by these compounds. Indeed, the length-to-width ratio of the dye-labeled area decreases by about half (e.g. 4.8 in DMSO controls versus 2.7 in SP600125 embryos; $P<0.001$) in inhibitor-treated embryos.

To assess radial intercalation, we labeled the central-most cells in the core of the primitive gut tube with deep DiI injections (Fig. 3I) and then exposed labeled embryos to DMSO, RO or SP600125. As expected, in DMSO controls these central endoderm cells radially redistribute such that they are all in contact with the basement membrane by stage 46 (Fig. 3J,J′). By contrast, the majority of central cells in both SP600125 (Fig. 3K,K′) and RO (Fig. 3L,L′) embryos fail to move outwards. However, careful examination of the abnormal labeling patterns reveals interesting differences between SP600125 and RO guts (Fig. 3M). For example, although labeled cells in RO-treated embryos often span the entire diameter of the tube (e.g. Fig. 3L,L′), this broad labeling pattern is not observed in SP600125 embryos (Fig. 3M). By contrast, labeled cells in SP600125 guts are sometimes confined to a small central core within the tube (e.g. Fig. 3K′), a distribution pattern not observed upon exposure to RO (Fig. 3M). These subtle distinctions suggest that, although both Rho kinase and JNK are required for the intercellular rearrangements that elongate the gut tube, they play different roles during this process.

JNK is required for endoderm cell adhesion

To distinguish the cellular roles of Rho kinase and JNK in gut morphogenesis, we compared epithelial architecture in the guts of RO- and SP600125-exposed embryos. In DMSO control guts, the endoderm becomes reorganized into a polarized epithelium, indicated by the enrichment of the apical marker aPKC at the lumenal surface and the cell-cell adhesion marker E-cadherin at basolateral membranes (Fig. 4A,D). In RO-exposed guts, aberrant foci of aPKC and E-cadherin (arrowheads, Fig. 4C,F) are found throughout the disorganized endoderm that occludes the tube.

In contrast to both DMSO- and RO-exposed embryos, guts exposed to SP600125 become sorted into two concentrically arranged, outer and inner, cell populations, separated by an irregular 'ring' of expression of aPKC (arrows, Fig. 4E). The outer cell population (i.e. exterior to the aPKC boundary) a highly disorganized, stratified epithelium, characterized by decreased localization of E-cadherin (Fig. 4B,E) and other forms adherens junction components (α- and β-catenin; supplementary material Fig. S1). Degradation and/or decreased levels of these proteins are also indicated by western blot analyses of gut extracts (Fig. 4G). The effects of JNK inhibition on cell-cell adhesion appear to be concentration dependent, and correlate with the severity of the short gut phenotype (supplementary material Fig. S2D,F,H,J); although the extent of RO-induced gut elongation defects is also concentration-dependent, the changes in adhesion and tissue architecture elicited by SP600125 are not observed in RO-exposed guts, regardless of concentration (supplementary material Fig. S2L,N,P,R)

The inner cell population in the SP600125-exposed embryo (i.e. interior to the aPKC boundary; asterisks in Fig. 4B,E) is loosely organized, and E-cadherin and other adherens junction components (Fig. 4B,E; supplementary material Fig. S1) are either undetectable or are associated with clumps of cell debris in this region, suggesting that the inner cells are largely nonadherent and may be undergoing programmed cell death. Apoptosis may be regulated by JNK activity in other contexts (Liu and Lin, 2005); however, activated caspase was not detected in the SP600125 gut endoderm prior to 48 hours exposure (stage 45; supplementary material Fig. S3G-L). By contrast, defects in E-cadherin were evident in SP600125 guts as early as 12 hours after exposure (stage 38; supplementary material Fig. S3A-F). These results indicate that decreased adhesion

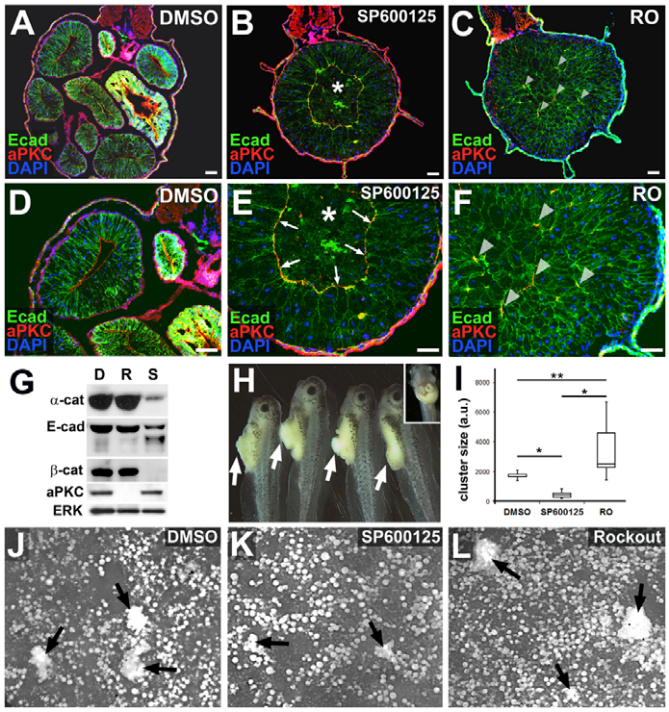

Fig. 4. JNK is required for endoderm cell adhesion. (**A-F**) Embryos were exposed to DMSO (A,D), SP600125 (B,E) or Rockout (RO; C,F) from stage 35-46 and transverse sections were immunohistochemically stained to reveal E-cadherin as a marker of cell-cell adhesion at basolateral membranes (Ecad, green), atypical protein kinase C as a marker of apical polarity (aPKC, red) and DAPI-stained nuclei (blue) in the developing gut tube. Compared with the mature epithelium found lining the sections of the elongated DMSO control gut, epithelial morphogenesis is severely disrupted in the shortened guts induced by exposure to SP600125 and RO. SP600125-exposed guts display a ring of aPKC (arrows, E) and generally reduced levels of E-cadherin (compare E with D,F), whereas RO guts possess aberrant foci of aPKC throughout the endoderm (arrowheads in C,F). Asterisks in B and E indicate the central core of unintercalated, non-adherent endoderm cells ('inner' population). (**G**) Western blot analyses confirm reduced levels of E-cadherin (Ecad), β-catenin (β-cat) and α-catenin (α-cat) in guts isolated from embryos exposed to SP600125 (S), compared with DMSO (D) and RO (R). By contrast, levels of aPKC are downregulated by exposure to RO, but unaffected by exposure to DMSO or SP600125. ERK, loading control. (**H**) Masses of loose endoderm cells (arrows) protrude from the guts of embryos exposed to SP600125 from stage 28-45, indicating defective tissue cohesion. (A DMSO control embryo is shown in the inset.) (**I-L**) Stage 46 guts were dissected from embryos exposed to DMSO (J), SP600125 (K) or Rockout (L) from stage 35 and dissociated into a single cell suspension in calcium- and magnesium-free medium; dissociated cells reaggregate into multicellular clusters upon reintroduction of calcium. The size (area) of cell clusters (arrows) derived from SP600125 guts is significantly smaller than clusters derived from DMSO or RO guts, indicating that SP600125 guts have decreased calcium-dependent (i.e. cadherin-based) cell-cell adhesion. By contrast, clusters derived from RO guts are significantly larger than DMSO or SP600125 clusters (I; n=10-22 clusters per condition). *P<0.01; **P<0.01. Each box plot is displayed as the median surrounded by a box representing the interquartile range; error bars indicate minimum and maximum values. Scale bars: 50 μm.

is a primary consequence of inhibiting JNK activity in the gut endoderm and that the isolated inner cell population subsequently undergoes cell death due to lack of adhesive contacts.

Consistent with a role for JNK in cell-cell adhesion, masses of loosely associated endoderm cells extrude out of the gut tube in embryos exposed to SP600125 for extended culture periods (Fig. 4H). In addition, dissociation-reaggregation assays with isolated gut cells – analogous to the standard assays performed to assess cell-cell adhesion in *Xenopus* animal cap cells (Sive et al., 2007; see Materials and methods) – provide additional functional evidence that JNK is required for cell-cell adhesion. In these assays, gut tubes from embryos exposed to DMSO, SP600125 and RO are dissociated into a single cell suspension by culturing them in the absence of divalent cations. The size of multicellular reaggregates formed after reintroducing Ca^{2+} ions to the culture medium provides an estimate of the strength of calcium-dependent (i.e. cadherin-mediated) intercellular adhesion (Fig. 4I-L). These assays indicated that cell-cell adhesion is significantly reduced (P<0.01) in SP600125 guts (relative to DMSO controls), and slightly increased in RO guts (Fig. 4I). Taken together, the above molecular, cellular and functional analyses strongly indicate that JNK activity is required to retain cell-cell adhesion in the elongating gut tube.

Morpholino knockdown of JNK1 results in loss of cell-cell adhesion

To validate genetically the role of JNK in gut morphogenesis, we injected a morpholino oligonucleotide (JNK1 MO) previously shown to specifically knock down translation of *Xenopus JNK1* and disrupt convergent extension (Liao et al., 2006; Yamanaka et al., 2002). To avoid potential off-target effects of JNK1 knockdown during gastrulation, we targeted our injections to the blastomeres of the early embryo that are fated to give rise (primarily) to the gut endoderm (Reed et al., 2009). Although injection of a control morpholino (Cont MO) rarely elicits gut defects (10%, n=87; Fig. 5A,B), injection of JNK1 MO results in severe inhibition of gut elongation (Fig. 5D,E; 53%, n=210; P<0.0001). Importantly, these phenotypes are accompanied by knockdown of JNK1 protein and decreased phosphoJun levels in gut extracts (Fig. 5C).

To ascertain the effect of JNK1 knockdown on cell-cell adhesion, we assessed tissue architecture in JNK1 MO-injected guts. Although Cont MO-injected endoderm cells (red cells in Fig. 5F,G) exhibit normal levels of E-cadherin (Fig. 5J,K) and form a columnar epithelium (Fig. 5N,O), the JNK1 MO-injected endoderm cells (red cells in Fig. 5H,I) exhibit dramatically decreased levels of E-cadherin (Fig. 5L,M) and are rounded and disorganized (Fig. 5P,Q). Moreover, similar to SP600125 guts, the JNK1 MO-injected cells form a nonadherent inner mass of endoderm that fills the gut lumen (asterisks, Fig. 5L,M). JNK1 activity is cell-autonomously required to retain cell-cell adhesion in this population, as neighboring uninjected endoderm cells in the same embryo possess normal levels of E-cadherin (compare injected and uninjected populations, separated by a broken line in Fig. 5M). These studies genetically validate the role of JNK in maintaining cell-cell contacts in the rearranging endoderm.

JNK is required for endoderm microtubule (MT) architecture

The rearrangement of the endoderm and elongation of the gut tube occur concomitantly with the morphogenesis of a polarized epithelium, a process that is known to be dependent on the remodeling and maturation of adhesive contacts, as described above, but also involves cytoskeletal reorganization. In developing organs, epithelial polarization and heightening are accompanied by dramatic microtubule (MT) reorganization, in which the dynamic, nonparallel MTs found in initially mesenchymal/migratory cells are reoriented into apicobasally aligned, linear arrays (Bartolini and Gundersen, 2006). This reorganization is observed during the

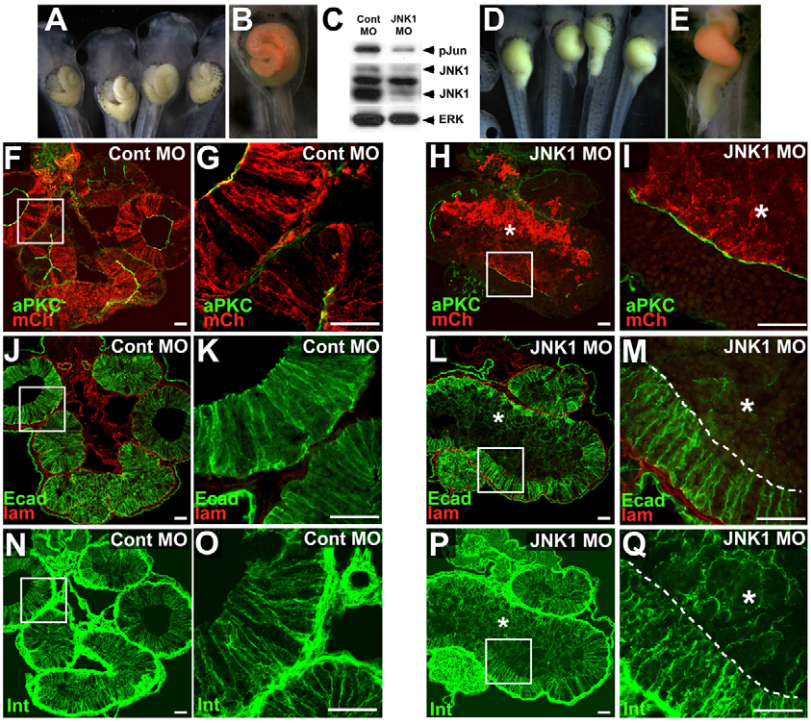

Fig. 5. Morpholino knockdown of JNK1 results in loss of cell-cell adhesion. (**A**,**B**,**D**,**E**) Embryos were injected with a control morpholino oligonucleotide (Cont MO; A,B,F,G,J,K,N,O) or a morpholino (MO) targeting *Xenopus JNK1* (JNK1 MO; D,E,H,I,L,M,P,Q). (**C**) Knockdown of JNK1 protein and JNK activity (phosphoJun) is evident in extracts from JNK MO-injected (mosaic) guts, compared with Cont MO-injected gut extracts. (B,E) MOs were co-injected with mCherry mRNA as a lineage tracer to confirm gut targeted injection (red). (**F-Q**) Sections of Cont or JNK MO-injected embryos reveal the localization of atypical protein kinase C and mCherry (aPKC, green; mCh, red; F-I), E-cadherin and laminin (Ecad, green; lam, red; J-M), and integrin-β1 (Int, green, to delineate cell outlines; N-Q) in the gut. Endoderm cells in stage 46 Cont MO-injected embryos (red cells in F-G) undergo normal intercalation and epithelial morphogenesis, as indicated by the single layer of columnar epithelial cells (N-O) with normal E-cadherin (J,K). By contrast, endoderm cells with MO-disrupted JNK1 function (red cells in H,I) do not radially intercalate or form a normal epithelium, as indicated by their irregular cell shapes (P,Q) and reduced levels of E-cadherin (L,M). Asterisks indicate an inner population of endoderm cells. (G,K,O,I,M,Q) Higher magnification images of boxed areas in F,J,N,H,L,P, respectively. Scale bars: 50 μm.

morphogenesis of the *Xenopus* gut epithelium as arrays of MTs become apicobasally oriented in the endoderm cells prior to and during intercalation (arrows, Fig. 6A,B,K). By stage 46, the MT network has reorganized into comet-like arrays emanating from the apical membrane of the polarized digestive epithelium (arrows, Fig. 6C,C′).

In the endoderm of embryos exposed to RO, apicobasally aligned MTs are also apparent (Fig. 6G,H,Q), although they eventually form disorganized foci (arrowheads, Fig. 6H-I′). By contrast, dramatically fewer MT arrays form in embryos exposed to SP600125 (Fig. 6D,E,N). Indeed, by stage 46, tubulin is virtually undetectable in the gut core (asterisks, Fig. 6F,F′) and only a few comet-like MT arrays are evident throughout the gut (arrows, Fig. 6F′). Earlier (stage 42), the few MTs detectable in SP600125 guts appear sparse compared with the DMSO and RO MT networks (arrows, Fig. 6K,N,Q). Moreover, although the MT arrays in DMSO and RO endoderm cells are predominantly apicobasally aligned in parallel, the MTs in the SP600125 endoderm are more disoriented (Fig. 6S-U).

This dependence of endoderm MT architecture on JNK activity was genetically validated by gut-targeted morpholino knockdown of *Xenopus JNK1*. Although Cont MO-injected endoderm cells exhibit normal MT architecture (supplementary material Fig. S4A-D), MT arrays in the JNK1 MO-injected endoderm are sparsely distributed and disorganized, especially in the non-adherent inner cell population (asterisks, supplementary material Fig. S4E-H). Taken together, these results show that JNK activity is required for proper polymerization and organization of parallel MT arrays in the gut endoderm.

Microtubule polymerization regulates cell adhesion in the gut endoderm

Microtubules (MTs) have recently emerged as key factors regulating the biogenesis, function and stability of cell-cell adhesive contacts during epithelial morphogenesis (Akhmanova et al., 2009). Therefore, we reasoned that the role of JNK in maintaining cell-cell adhesion during endoderm rearrangement might be mediated by its dramatic effect on MT organization. If so, then directly perturbing MT architecture during gut elongation may be expected to phenocopy the effects of JNK inhibition.

To test this hypothesis, we exposed embryos to nocodazole, a small-molecule inhibitor of MT polymerization. Embryos were exposed from stage 35 to stage 41, to perturb the initial formation of polymerized MT arrays in the gut endoderm, as chronic exposure to nocodazole throughout gut morphogenesis proved toxic (not shown). This limited nocodazole exposure led to severe shortening of the gut tube in most embryos (95%; n=22; Fig. 7A,H), comparable with that induced by exposure to SP600125 (see Fig. 2B). At the cellular level, the depletion of polymerized MTs by nocodazole results in a tissue dissociation phenotype that is strikingly similar to that elicited by SP600125. Indeed, in contrast to the single-layer epithelium evident in fully lengthened control guts (Fig. 7B-G), the endoderm in guts exposed to nocodazole becomes sorted into two concentrically arranged, outer and inner, cell populations (Fig. 7I-N), as observed with JNK inhibition (see Fig. 4). Moreover, although some β-catenin staining is evident in the outer layer, it is largely undetectable in the innermost cells (asterisks in Fig. 7I,L), another characteristic feature of SP600125-exposed guts (see supplementary material Fig. S1). These results show that several key effects of SP600125 on cell-cell adhesion and gut tissue architecture are phenocopied by disrupting MT polymerization, independent of any direct manipulation of JNK itself. Interestingly, these defects are not observed in the presence of mitotic inhibitors that aberrantly stabilize MTs (e.g. epothilone; supplementary material Fig. S5), suggesting that it is not MT dynamics, but the stability of the MT architecture, that is required to maintain adhesive contacts in the rearranging endoderm.

JNK does not regulate actin polymerization in the gut endoderm

MT stability and cadherin-dependent cell-cell adhesion are mutually interdependent, but these properties can also affect, and

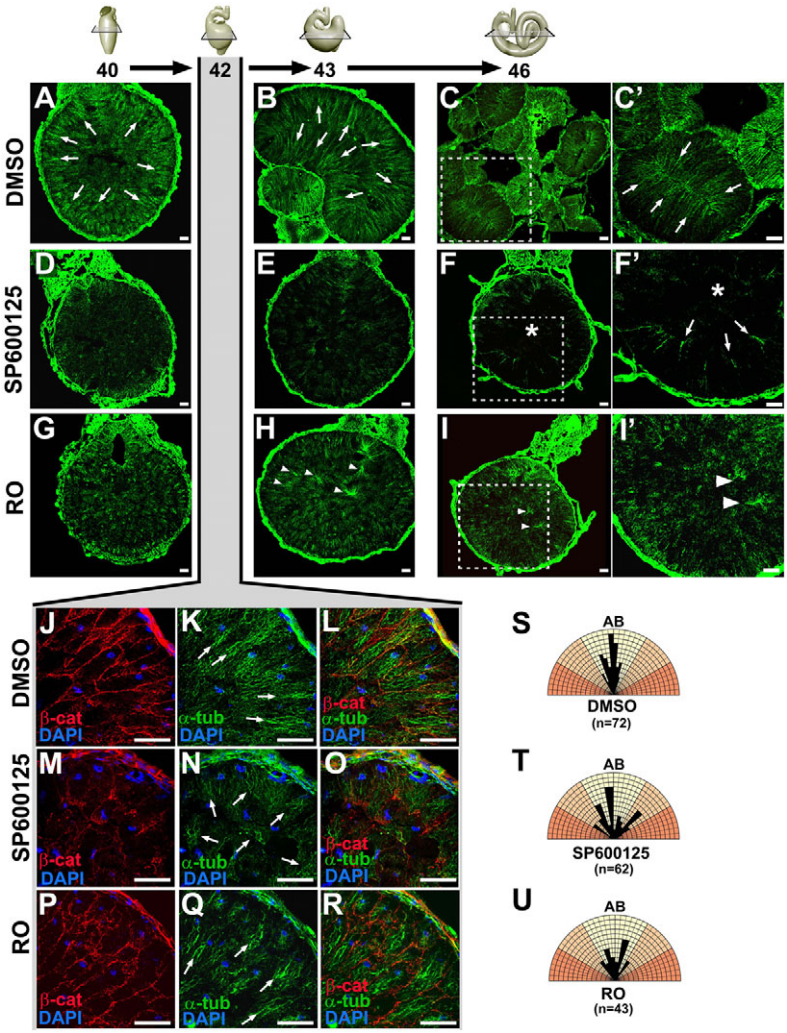

Fig. 6. JNK is required for endoderm microtubule (MT) architecture. (**A-R**) Embryos were exposed to DMSO (A-C′,J-L), SP600125 (D-F′,M-O) or Rockout (RO; G-I′,P-R) from stage 35 through to stage 40 (A,D,G), 42 (J-R), 43 (B,E,H) or 46 (C,C′,F,F′,I,I′), and transverse sections were stained with α-tubulin (green) to reveal MT architecture, β-catenin (red) to indicate cell-cell adhesive contacts and/or DAPI to show nuclei (blue). (C′,F′,I′) Higher magnification images of the boxed areas in C,F,I, respectively. Apicobasally oriented MT arrays (arrows) are evident in DMSO control guts (A-C′,K), but MT polymerization is disrupted in the presence of SP600125 (D-F′,N), especially in the inner cell population (asterisks, F,F′). Although MT arrays are predominantly apicobasally oriented in RO guts at stage 42 (Q), abnormal foci of MTs eventually form throughout the gut (arrowheads, H-I′). (**S-U**) Polar coordinate diagrams show the orientation of the MTs in DMSO, SP600125 and RO guts (stage 42). Black bars show the alignment of individual MTs with respect to the apicobasal axis (AB) of the relevant cell, whereas the length of the bar indicates the relative numbers of MTs oriented at that angle. Bars in yellow sectors indicate MTs oriented within 30° of the apicobasal axis, whereas bars in orange sectors indicate MTs that deviated outside of this region. In DMSO (S) and RO (U) guts, most MTs are oriented in parallel (within the yellow sectors); however, the angles of individual MTs are more variable in guts exposed to SP600125 (T). Scale bars: 50 μm.

be affected by, the state of actin polymerization (Harris and Tepass, 2010; Niessen et al., 2011). Interestingly, JNK can regulate the assembly of actin during morphogenesis (Xia and Karin, 2004), suggesting that the role of JNK in endoderm rearrangement might also involve actin assembly. Somewhat consistent with this idea, we found that, at end-stage, the inner endoderm cell population of SP600125-treated guts lacked the polymerized cortical actin found in controls (supplementary material Fig. S6A-F′). However, the outer population retained cortical actin and formed a circumferential actin belt at the apical surface of the abnormal epithelium (supplementary material Fig. S6D-F), suggesting that actin polymerization *per se* is not hindered in the absence of JNK activity. Rather, the absence of polymerized actin in the core of the gut tube at this stage is more likely to be a secondary consequence of the paucity of actin-stabilizing adhesive contacts in the apoptotic inner cell population.

To further assess whether adhesion, MTs or actin may be the primary target of JNK activity, we assessed SP600125 guts at earlier stages of exposure. Defects in β-catenin distribution and MT organization were found to occur within 8 hours of adding the JNK inhibitor (supplementary material Fig. S6G-R). However, we could not detect an effect on cortical actin with this treatment (supplementary material Fig. S6S-X), confirming that regulation of actin polymerization is not the primary morphogenetic role of JNK during gut elongation.

Taken together, our data are consistent with a model in which JNK signaling influences MT dynamics to maintain cell-cell adhesion during the radial intercalation of the endoderm that drives epithelial morphogenesis and tissue elongation in the *Xenopus* gut tube.

DISCUSSION

The cellular morphogenetic mechanisms that underlie primitive gut tube elongation are poorly understood. Elucidating these mechanisms is crucial for deciphering the developmental processes that shape both normal and abnormal digestive tract topologies across species. The results presented herein reveal novel roles for Jun N-terminal kinase (JNK) in the rearrangement of the gut endoderm that drives gut elongation.

JNK maintains cell-cell adhesion during endoderm rearrangements

During morphogenesis, intercellular adhesive contacts must be flexible enough to permit rearrangement while still maintaining overall tissue integrity. It is well established that Rho GTPase controls actomyosin contractility to power the shape change and adhesive remodeling necessary to reorganize embryonic tissues (Patwari and Lee, 2008). Indeed, when Rho kinase activity is inhibited in the developing gut, endoderm cells remain largely immotile, precluding gut lengthening (Reed et al., 2009). The

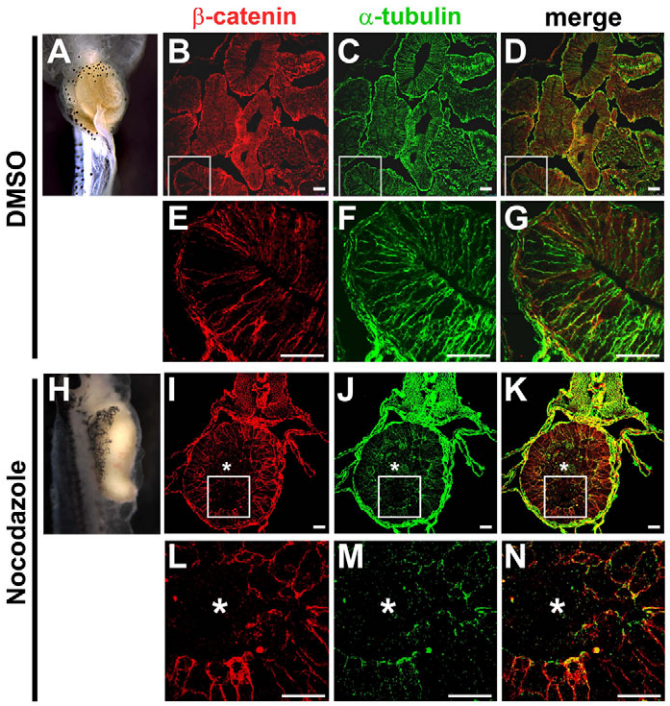

Fig. 7. Microtubule polymerization regulates endoderm adhesion. (**A-N**) Embryos were exposed to DMSO (A-G) or nocodazole (H-N) during the stages prior to gut elongation (stage 35-41), and recovered in normal medium through stage 46. Compared with DMSO controls (A), nocodazole exposure perturbs gut elongation (H). Transverse sections were stained for β-catenin (red, cell-cell adhesion; B,E,I,L) and α-tubulin (green, MTs; C,F,J,M), with merged (red-green) images shown in D,G,K,N. Compared with the mature epithelium found lining the elongated gut tube of DMSO controls (B-G), epithelial morphogenesis is severely disrupted in the shortened guts induced by exposure to nocodazole (I-N). Endoderm cells are deficient in both MTs and β-catenin, and sort into inner (asterisks) and outer populations. Scale bars: 50 μm.

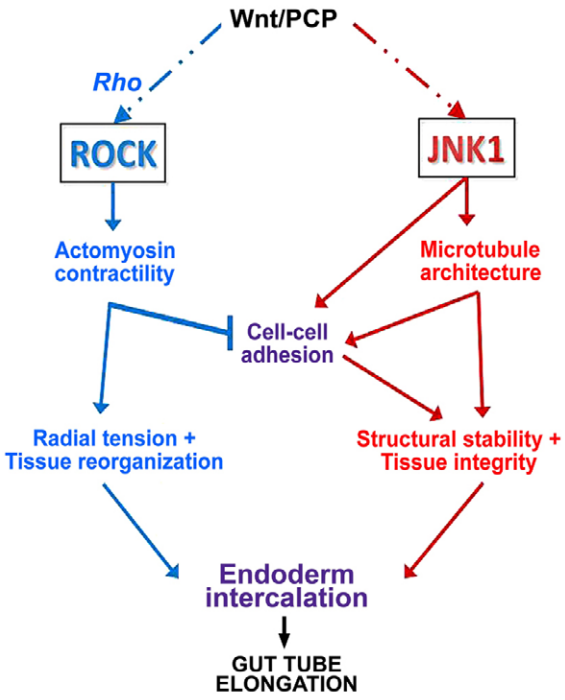

Fig. 8. Model of the complementary roles of ROCK and JNK in gut elongation. Rho activates actomyosin-based contractility via Rho kinase (ROCK) to generate tension and remodel cadherin-based cell-cell adhesive contacts, leading to the radial reorganization of the gut endoderm (blue arrows). By contrast, JNK signaling stabilizes cell-cell adhesion, either directly and/or via its effects on microtubule architecture (red arrows), to maintain structural integrity during endoderm rearrangement. Both pathways must be coordinated in space and time, within and between cells, to control cell intercalation events in order to achieve anisotropic tissue extension to elongate the gut tube. See text for further details.

present study demonstrates that the gut also fails to elongate when JNK activity is abrogated; however, rather than remaining fixed, the adhesive interactions between JNK-deficient endoderm cells are too weak. This defect also impedes tissue lengthening because the central cells do not retain sufficient adhesive contacts to intercalate and form an epithelium; instead, they dissociate and become sorted from the rest of the population. Thus, JNK signaling ensures the necessary tissue cohesion to allow all the endoderm cells to radially intercalate and impel gut tube extension.

This novel function of JNK in gut elongation is consistent with the general role of this molecule in preserving the communication and cohesion between neighboring cells in other contexts (Xia and Karin, 2004). For example, JNK maintains intercellular adhesivity during *Drosophila* thorax closure; in JNK pathway mutants, normally cohesive cell populations dissociate and undergo premature cell death, similar to our observations of the endoderm in JNK-deficient guts (Martín-Blanco et al., 2000). Likewise, in the *Drosophila* ovary, JNK maintains cell-cell adhesive contacts between border cells to sustain the intercellular contacts necessary for their collective migration (Wang et al., 2010). Here too, as we observed in the JNK-deficient gut, E-cadherin and β-catenin are downregulated when JNK function is disrupted (Llense and Martín-Blanco, 2008; Wang et al., 2010). The role of JNK in maintaining cell adhesion during gut elongation is thus consistent with the known functions of this molecule in a diverse array of morphogenetic events across species.

JNK regulates microtubule architecture during endoderm rearrangements

An intriguing finding of this study is that JNK activity is required for the formation of parallel MT arrays within rearranging endoderm cells during gut elongation. MTs are also required for the convergent extension movements of gastrulation (Lane and Keller, 1997; Sepich et al., 2011; Shindo et al., 2008), although it is unknown whether JNK signaling influences MT architecture in this context. Nonetheless, JNK plays pivotal roles in MT organization and stability in other cell types. For example, during neurogenesis, JNK regulates the bundling of MTs into parallel arrays to stabilize neurite structure and elongate axons (Horton and Ehlers, 2003; Maccioni and Cambiazo, 1995; Signor and Scholey, 2000).

Intriguingly, we found that depleting polymerized MTs with nocodazole phenocopies many of the effects of JNK inhibition on gut morphogenesis, including perturbing cell-cell adhesion. This result is consistent with the known roles of MTs in the generation, maintenance and local concentration of cell-cell adhesive contacts not only in differentiating epithelia (Akhmanova et al., 2009; Harris and Tepass, 2010; Meng and Takeichi, 2009; Stehbens et al., 2006; Stehbens et al., 2009), but also in mesoderm cells undergoing

convergent extension (Kwan and Kirschner, 2005; Lane and Keller, 1997). Although we cannot rule out the possibility that JNK exerts a direct effect on adherens junction protein expression or phosphorylation state (e.g. Lee et al., 2009), our nocodazole data suggest that JNK may, at least in part, regulate cell-cell adhesion in the gut endoderm via its effects on MT architecture (see Fig. 8).

JNK and Rho kinase play complementary roles in gut elongation

Xenopus gut elongation provides a novel paradigm for understanding the general roles of Rho kinase and JNK during tissue-elongating cell rearrangement. Our results suggest a model in which, by maintaining microtubule architecture within cells, and adhesive contacts between cells, JNK activation balances the Rho kinase-mediated tensile forces that direct endoderm rearrangement (Fig. 8). This is consistent with the known roles of actomyosin contraction in force production, the role of cell adhesion in force transmission, and the ability of MTs to resist tension and bear compression to stabilize cell shape and tissue stiffness (Kaverina and Straube, 2011; Nagayama and Matsumoto, 2008; Wang, 1998; Wang et al., 2001).

This Rho kinase/JNK dichotomy must be properly balanced to coordinate gut elongation with digestive epithelial morphogenesis. How might this balance be achieved? Our simplified model portrays the roles of Rho kinase and JNK in parallel, but these two pathways must, of course, be continually integrated in space and time to smoothly orchestrate the cytoskeletal and adhesive dynamics underlying cell rearrangement. Although Rho kinase and JNK may be independently activated, Rho signaling can also function upstream of, or parallel with JNK activation (Kim and Han, 2005; Unterseher et al., 2004), providing a means of direct signal integration. Reciprocally, MT-associated guanine nucleotide exchange factors (GEFs) can signal to actomyosin through Rho GTPases (Kwan and Kirschner, 2005; Lane and Keller, 1997; Nalbant et al., 2009), and MT disruption can activate actomyosin contraction to increase cellular tension (Elbaum et al., 1999; Kolodney and Elson, 1995; Stamenović et al., 2002). Future studies will help elucidate the upstream activators and downstream targets of JNK in gut elongation – with larger implications for a variety of morphogenetic cell rearrangement events that shape elongated tubes, organs and body plans.

Implications for gut digestive organ defects and gut evolution

The results presented herein shed new light on the mechanisms of gut elongation, revealing a mechanistic relationship between endoderm rearrangements, epithelial morphogenesis and tissue lengthening regulated by Rho kinase and JNK. A similar association is likely to underlie gut elongation in other vertebrates, as intriguing similarities exist between SP600125- and RO-treated *Xenopus* guts and the shortened guts of Wnt/PCP mutant mice, including defective epithelial architecture, the presence of apoptotic cell masses in the lumen and an increased tube diameter (Cervantes et al., 2009; Matsuyama et al., 2009; Yamada et al., 2010). In humans, congenital defects in gut length are often associated with other gut deformities, including intestinal stenoses, atresias and/or malrotations (Chu et al., 2004; Hasosah et al., 2008; Kern et al., 1990; Martucciello et al., 2002; Palle and Reddy, 2010; Sabharwal et al., 2004; Sansaricq et al., 1984; Schalamon et al., 1999), suggesting that the mechanisms underlying gut elongation, including the potential roles of Rho kinase and JNK, may be highly relevant to the etiology of common human deformities.

Acknowledgements
We are grateful to members of N.N.-Y.'s laboratory, and to J. Yoder and T. Ghashghaei for helpful comments on the manuscript. Some antibodies were provided by the NIH-supported DSHB.

Funding
This work was funded by a grant to N.N.-Y. from the National Institutes of Health [5R01DK085300]. Deposited in PMC for release after 12 months.

Competing interests statement
The authors declare no competing financial interests.

Supplementary material
Supplementary material available online at
http://dev.biologists.org/lookup/suppl/doi:10.1242/dev.086850/-/DC1

References

Akhmanova, A., Stehbens, S. J. and Yap, A. S. (2009). Touch, grasp, deliver and control: functional cross-talk between microtubules and cell adhesions. *Traffic* **10**, 268-274.
Bartolini, F. and Gundersen, G. G. (2006). Generation of noncentrosomal microtubule arrays. *J. Cell Sci.* **119**, 4155-4163.
Bennett, B. L., Sasaki, D. T., Murray, B. W., O'Leary, E. C., Sakata, S. T., Xu, W., Leisten, J. C., Motiwala, A., Pierce, S., Satoh, Y. et al. (2001). SP600125, an anthrapyrazolone inhibitor of Jun N-terminal kinase. *Proc. Natl. Acad. Sci. USA* **98**, 13681-13686.
Boutros, M., Paricio, N., Strutt, D. I. and Mlodzik, M. (1998). Dishevelled activates JNK and discriminates between JNK pathways in planar polarity and wingless signaling. *Cell* **94**, 109-118.
Carron, C., Bourdelas, A., Li, H. Y., Boucaut, J. C. and Shi, D. L. (2005). Antagonistic interaction between IGF and Wnt/JNK signaling in convergent extension in Xenopus embryo. *Mech. Dev.* **122**, 1234-1247.
Cervantes, S., Yamaguchi, T. P. and Hebrok, M. (2009). Wnt5a is essential for intestinal elongation in mice. *Dev. Biol.* **326**, 285-294.
Chalmers, A. D. and Slack, J. M. (2000). The Xenopus tadpole gut: fate maps and morphogenetic movements. *Development* **127**, 381-392.
Chu, S. M., Luo, C. C., Chou, Y. H. and Yen, J. B. (2004). Congenital short bowel syndrome with malrotation. *Chang Gung Med. J.* **27**, 548-550.
Elbaum, M., Chausovsky, A., Levy, E. T., Shtutman, M. and Bershadsky, A. D. (1999). Microtubule involvement in regulating cell contractility and adhesion-dependent signalling: a possible mechanism for polarization of cell motility. *Biochem. Soc. Symp.* **65**, 147-172.
García-García, M. J., Shibata, M. and Anderson, K. V. (2008). Chato, a KRAB zinc-finger protein, regulates convergent extension in the mouse embryo. *Development* **135**, 3053-3062.
Grosse, A. S., Pressprich, M. F., Curley, L. B., Hamilton, K. L., Margolis, B., Hildebrand, J. D. and Gumucio, D. L. (2011). Cell dynamics in fetal intestinal epithelium: implications for intestinal growth and morphogenesis. *Development* **138**, 4423-4432.
Habas, R., Dawid, I. B. and He, X. (2003). Coactivation of Rac and Rho by Wnt/Frizzled signaling is required for vertebrate gastrulation. *Genes Dev.* **17**, 295-309.
Harris, T. J. and Tepass, U. (2010). Adherens junctions: from molecules to morphogenesis. *Nat. Rev. Mol. Cell Biol.* **11**, 502-514.
Hasosah, M., Lemberg, D. A., Skarsgard, E. and Schreiber, R. (2008). Congenital short bowel syndrome: a case report and review of the literature. *Can. J. Gastroenterol.* **22**, 71-74.
Horton, A. C. and Ehlers, M. D. (2003). Neuronal polarity and trafficking. *Neuron* **40**, 277-295.
Jones, C. and Chen, P. (2007). Planar cell polarity signaling in vertebrates. *Bioessays* **29**, 120-132.
Karasov, W. H. and Diamond, J. M. (1988). Interplay between physiology and ecology in digestion. *Bioscience* **38**, 602-611.
Kaverina, I. and Straube, A. (2011). Regulation of cell migration by dynamic microtubules. *Semin. Cell Dev. Biol.* **22**, 968-974.
Keller, R. (2002). Shaping the vertebrate body plan by polarized embryonic cell movements. *Science* **298**, 1950-1954.
Kern, I. B., Leece, A. and Bohane, T. (1990). Congenital short gut, malrotation, and dysmotility of the small bowel. *J. Pediatr. Gastroenterol. Nutr.* **11**, 411-415.
Kim, G. H. and Han, J. K. (2005). JNK and ROKalpha function in the noncanonical Wnt/RhoA signaling pathway to regulate Xenopus convergent extension movements. *Dev. Dyn.* **232**, 958-968.
Kolodney, M. S. and Elson, E. L. (1995). Contraction due to microtubule disruption is associated with increased phosphorylation of myosin regulatory light chain. *Proc. Natl. Acad. Sci. USA* **92**, 10252-10256.
Kwan, K. M. and Kirschner, M. W. (2005). A microtubule-binding Rho-GEF controls cell morphology during convergent extension of Xenopus laevis. *Development* **132**, 4599-4610.

Lane, M. C. and Keller, R. (1997). Microtubule disruption reveals that Spemann's organizer is subdivided into two domains by the vegetal alignment zone. *Development* **124**, 895-906.
Lee, M. H., Koria, P., Qu, J. and Andreadis, S. T. (2009). JNK phosphorylates beta-catenin and regulates adherens junctions. *FASEB J.* **23**, 3874-3883.
Li, Y., Rankin, S. A., Sinner, D., Kenny, A. P., Krieg, P. A. and Zorn, A. M. (2008). Sfrp5 coordinates foregut specification and morphogenesis by antagonizing both canonical and noncanonical Wnt11 signaling. *Genes Dev.* **22**, 3050-3063.
Liao, G., Tao, Q., Kofron, M., Chen, J. S., Schloemer, A., Davis, R. J., Hsieh, J. C., Wylie, C., Heasman, J. and Kuan, C. Y. (2006). Jun NH2-terminal kinase (JNK) prevents nuclear beta-catenin accumulation and regulates axis formation in Xenopus embryos. *Proc. Natl. Acad. Sci. USA* **103**, 16313-16318.
Lipscomb, K., Schmitt, C., Sablyak, A., Yoder, J. A. and Nascone-Yoder, N. (2006). Role for retinoid signaling in left-right asymmetric digestive organ morphogenesis. *Dev. Dyn.* **235**, 2266-2275.
Liu, J. and Lin, A. (2005). Role of JNK activation in apoptosis: a double-edged sword. *Cell Res.* **15**, 36-42.
Llense, F. and Martín-Blanco, E. (2008). JNK signaling controls border cell cluster integrity and collective cell migration. *Curr. Biol.* **18**, 538-544.
Maccioni, R. B. and Cambiazo, V. (1995). Role of microtubule-associated proteins in the control of microtubule assembly. *Physiol. Rev.* **75**, 835-864.
Marlow, F., Topczewski, J., Sepich, D. and Solnica-Krezel, L. (2002). Zebrafish Rho kinase 2 acts downstream of Wnt11 to mediate cell polarity and effective convergence and extension movements. *Curr. Biol.* **12**, 876-884.
Martín-Blanco, E., Pastor-Pareja, J. C. and Garcia-Bellido, A. (2000). JNK and decapentaplegic signaling control adhesiveness and cytoskeleton dynamics during thorax closure in Drosophila. *Proc. Natl. Acad. Sci. USA* **97**, 7888-7893.
Martucciello, G., Torre, M., Pini Prato, A., Lerone, M., Campus, R., Leggio, S. and Jasonni, V. (2002). Associated anomalies in intestinal neuronal dysplasia. *J. Pediatr. Surg.* **37**, 219-223.
Matsumoto, A., Hashimoto, K., Yoshioka, T. and Otani, H. (2002). Occlusion and subsequent re-canalization in early duodenal development of human embryos: integrated organogenesis and histogenesis through a possible epithelial-mesenchymal interaction. *Anat. Embryol. (Berl.)* **205**, 53-65.
Matsuyama, M., Aizawa, S. and Shimono, A. (2009). Sfrp controls apicobasal polarity and oriented cell division in developing gut epithelium. *PLoS Genet.* **5**, e1000427.
Meng, W. and Takeichi, M. (2009). Adherens junction: molecular architecture and regulation. *Cold Spring Harb. Perspect. Biol.* **1**, a002899.
Muller, J. K., Prather, D. R. and Nascone-Yoder, N. M. (2003). Left-right asymmetric morphogenesis in the Xenopus digestive system. *Dev. Dyn.* **228**, 672-682.
Nagayama, K. and Matsumoto, T. (2008). Contribution of actin filaments and microtubules to quasi-in situ tensile properties and internal force balance of cultured smooth muscle cells on a substrate. *Am. J. Physiol. Cell Physiol.* **295**, C1569-C1578.
Nalbant, P., Chang, Y. C., Birkenfeld, J., Chang, Z. F. and Bokoch, G. M. (2009). Guanine nucleotide exchange factor-H1 regulates cell migration via localized activation of RhoA at the leading edge. *Mol. Biol. Cell* **20**, 4070-4082.
Nandadasa, S., Tao, Q., Menon, N. R., Heasman, J. and Wylie, C. (2009). N- and E-cadherins in Xenopus are specifically required in the neural and non-neural ectoderm, respectively, for F-actin assembly and morphogenetic movements. *Development* **136**, 1327-1338.
Narumiya, S., Tanji, M. and Ishizaki, T. (2009). Rho signaling, ROCK and mDia1, in transformation, metastasis and invasion. *Cancer Metastasis Rev.* **28**, 65-76.
Niessen, C. M., Leckband, D. and Yap, A. S. (2011). Tissue organization by cadherin adhesion molecules: dynamic molecular and cellular mechanisms of morphogenetic regulation. *Physiol. Rev.* **91**, 691-731.
Nieuwkoop, P. D. and Faber, J. (1994). *Normal Table of Xenopus Laevis (Daudin)*. New York, NY: Garland Publishing Inc.
Palle, L. and Reddy, B. (2010). Case report: congenital short bowel syndrome. *Indian J. Radiol. Imaging* **20**, 227-229.
Patwari, P. and Lee, R. T. (2008). Mechanical control of tissue morphogenesis. *Circ. Res.* **103**, 234-243.
Reed, R. A., Womble, M. A., Dush, M. K., Tull, R. R., Bloom, S. K., Morckel, A. R., Devlin, E. W. and Nascone-Yoder, N. M. (2009). Morphogenesis of the primitive gut tube is generated by Rho/ROCK/myosin II-mediated endoderm rearrangements. *Dev. Dyn.* **238**, 3111-3125.
Roszko, I., Sawada, A. and Solnica-Krezel, L. (2009). Regulation of convergence and extension movements during vertebrate gastrulation by the Wnt/PCP pathway. *Semin. Cell Dev. Biol.* **20**, 986-997.
Sabharwal, G., Strouse, P. J., Islam, S. and Zoubi, N. (2004). Congenital short-gut syndrome. *Pediatr. Radiol.* **34**, 424-427.
Sansaricq, C., Chen, W. J., Manka, M., Davis, D. and Snyderman, S. (1984). Familial congenital short small bowel with associated defects. A long-term survival. *Clin. Pediatr. (Phila.)* **23**, 453-455.
Schalamon, J., Schober, P. H., Gallippi, P., Matthyssens, L. and Höllwarth, M. E. (1999). Congenital short-bowel; a case study and review of the literature. *Eur. J. Pediatr. Surg.* **9**, 248-250.
Sepich, D. S., Usmani, M., Pawlicki, S. and Solnica-Krezel, L. (2011). Wnt/PCP signaling controls intracellular position of MTOCs during gastrulation convergence and extension movements. *Development* **138**, 543-552.
Shindo, A., Yamamoto, T. S. and Ueno, N. (2008). Coordination of cell polarity during Xenopus gastrulation. *PLoS. ONE* **3,** e1600.
Signor, D. and Scholey, J. M. (2000). Microtubule-based transport along axons, dendrites and axonemes. *Essays Biochem.* **35**, 89-102.
Sive, H. L., Grainger, R. M. and Harland, R. M. (1998). *Early Development of Xenopus laevis*. New York, NY: Cold Spring Harbor Laboratory Press.
Sive, H. L., Grainger, R. M. and Harland, R. M. (2007). Dissociation and reaggregation of *Xenopus laevis* animal caps. *Cold Spring Harb. Protoc.* doi:10.1101/pdb.prot4745
Stainier, D. Y. (2005). No organ left behind: tales of gut development and evolution. *Science* **307**, 1902-1904.
Stamenović, D., Mijailovich, S. M., Tolić-Nørrelykke, I. M., Chen, J. and Wang, N. (2002). Cell prestress. II. Contribution of microtubules. *Am. J. Physiol. Cell Physiol.* **282**, C617-C624.
Stehbens, S. J., Paterson, A. D., Crampton, M. S., Shewan, A. M., Ferguson, C., Akhmanova, A., Parton, R. G. and Yap, A. S. (2006). Dynamic microtubules regulate the local concentration of E-cadherin at cell-cell contacts. *J. Cell Sci.* **119**, 1801-1811.
Stehbens, S. J., Akhmanova, A. and Yap, A. S. (2009). Microtubules and cadherins: a neglected partnership. *Front. Biosci.* **14**, 3159-3167.
Unterseher, F., Hefele, J. A., Giehl, K., De Robertis, E. M., Wedlich, D. and Schambony, A. (2004). Paraxial protocadherin coordinates cell polarity during convergent extension via Rho A and JNK. *EMBO J.* **23**, 3259-3269.
van Amerongen, R. and Nusse, R. (2009). Towards an integrated view of Wnt signaling in development. *Development* **136**, 3205-3214.
Wang, N. (1998). Mechanical interactions among cytoskeletal filaments. *Hypertension* **32**, 162-165.
Wang, N., Naruse, K., Stamenović, D., Fredberg, J. J., Mijailovich, S. M., Tolić-Nørrelykke, I. M., Polte, T., Mannix, R. and Ingber, D. E. (2001). Mechanical behavior in living cells consistent with the tensegrity model. *Proc. Natl. Acad. Sci. USA* **98**, 7765-7770.
Wang, X., He, L., Wu, Y. I., Hahn, K. M. and Montell, D. J. (2010). Light-mediated activation reveals a key role for Rac in collective guidance of cell movement in vivo. *Nat. Cell Biol.* **12**, 591-597.
Weaver, L. T., Austin, S. and Cole, T. J. (1991). Small intestinal length: a factor essential for gut adaptation. *Gut* **32**, 1321-1323.
Xia, Y. and Karin, M. (2004). The control of cell motility and epithelial morphogenesis by Jun kinases. *Trends Cell Biol.* **14**, 94-101.
Yamada, M., Udagawa, J., Matsumoto, A., Hashimoto, R., Hatta, T., Nishita, M., Minami, Y. and Otani, H. (2010). Ror2 is required for midgut elongation during mouse development. *Dev. Dyn.* **239**, 941-953.
Yamanaka, H., Moriguchi, T., Masuyama, N., Kusakabe, M., Hanafusa, H., Takada, R., Takada, S. and Nishida, E. (2002). JNK functions in the non-canonical Wnt pathway to regulate convergent extension movements in vertebrates. *EMBO Rep.* **3**, 69-75.
Yin, C., Kiskowski, M., Pouille, P. A., Farge, E. and Solnica-Krezel, L. (2008). Cooperation of polarized cell intercalations drives convergence and extension of presomitic mesoderm during zebrafish gastrulation. *J. Cell Biol.* **180**, 221-232.